

DOI: 10.1002/cctc.201200522

The Impact of Reaction Pressure on the Catalytic Performance of the Pd–Sb/TiO₂ Catalyst in the Acetoxylation of Toluene into Benzyl Acetate

Neetika Madaan, Suresh Gatla, Venkata Narayana Kalevaru, Jörg Radnik, Marga-Martina Pohl, Bernhard Lücke, Angelika Brückner, and Andreas Martin^{*[a]}

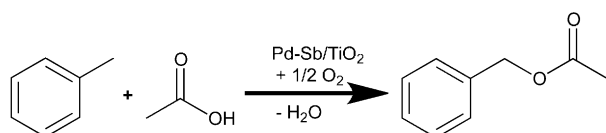
The acetoxylation of toluene in the presence of acetic acid and oxygen was performed over a Pd–Sb/TiO₂ catalyst at 210 °C and at various reaction pressures (1–10 bar). A remarkable improvement in the catalytic performance and a significant shortening of the induction period were found with an increase in pressure. At a pressure of 6 bar, the highest toluene conversion

of 75% and 100% selectivity for benzyl acetate were observed. This result could be due to both the restructuring of the catalyst surface and to the formation of active Pd–Sb particles of desired size, composition, and shape during the course of the induction period. Samples of the most-active and spent catalysts were studied by ex situ and in situ XRD, XPS, and TEM.

1. Introduction

Over the past two decades, the Pd-catalyzed oxidation of α -olefins and alkyl-aromatic compounds has become an increasingly attractive field and, in some instances, it is the only route for the selective synthesis of vinylic, allylic, and benzylic alcohols and esters. In this context, the development of more-effective and more-economic syntheses of benzylic esters/alcohols and even aldehydes as intermediates will be of great interest for the synthesis of various industrially important chemicals.

The acetoxylation of toluene (Tol) is a one-step process for the synthesis of benzyl acetate (BA) in the presence of acetic acid and oxygen (Scheme 1). Palladium-containing catalysts are



Scheme 1. The synthesis of benzylacetate.

widely used in various acetoxylation reactions, such as the manufacture of vinyl acetate monomer (VAM) from ethylene.^[1,2] Besides olefins, aromatic compounds, such as toluene, can be converted over Pd-containing catalysts in the same way.^[3–6] BA is naturally found in the odorous substances of various plants; therefore, it is mainly used in the perfume and

food industry, owing to its fruity aroma. BA is also notably used in the chemical industry as a solvent for the manufacture of cellulose acetate.^[7] The global demand for BA ranges from 5–10 kt per annum. In addition, in the future, it could serve as an intermediate for the manufacture of benzyl alcohol that is presently obtained by the rather harmful chlorination of toluene into benzyl chloride and subsequent hydrolysis.

From previous investigations,^[8–10] it has been observed that the performance of the acetoxylation reaction is strongly dependent on different parameters, such as Pd-particle size, the nature of the support, the type of the promoters (Sb seems to be the most beneficial), the preparation method, the calcination atmosphere, etc. Of these parameters, the size of the Pd particles has shown a strong influence on the catalytic performance, that is, 50–100 nm particles were found to exhibit better performance than smaller ones. It looks that this critical size, that is, a defined ensemble of Pd atoms, is needed to reach sufficient conversion and product selectivity. The catalyst only exhibits maximum activity at this critical size, which is reached after an induction period of 7–50 h, depending on the catalyst precursor that is used and its conditioning prior to the reaction.^[11,12] In addition, various investigations have led to the conclusion that a defined Pd/promoter surface-atom ratio seems to be advantageous (in the case of Sb, the Pd/Sb ratio is 5:1).^[10] Furthermore, catalyst deactivation is observed after a steady-state operating period, owing to surface reduction of PdO into Pd and Pd^{δ-} species and coking, respectively.^[11,12] Regeneration at 300 °C approximately restores the concentration of PdO but, at 350 °C, the PdO portion on the surface remains very low. In addition, Pd⁰, PdO, and Sb synergy is needed for a stable and high performance of the catalyst.

In general, the reaction is performed at a mild reaction temperature of about 210 °C and at a modest pressure of 2 bar. Pressure effects in catalysis are widely known from detailed

[a] Dr. N. Madaan, Dr. S. Gatla, Dr. V. N. Kalevaru, Dr. J. Radnik, Dr. M.-M. Pohl, Prof. B. Lücke, Prof. A. Brückner, Dr. A. Martin
Leibniz-Institut für Katalyse e. V. an
der Universität Rostock
Albert-Einstein-Str. 29a, 18059 Rostock (Germany)
Fax: (+49) 0381-1281-51246
E-mail: andreas.martin@catalysis.de

studies, for example, for changing the product distribution in the Fischer–Tropsch synthesis over Nb-supported Co-containing catalysts.^[13] Other examples might be the effect of pressure on the conversion of MeOH over zeolites^[14] or the impact of reaction pressure on the thermal and catalytic cracking of industrial feedstock and coke formation in catalytic cracking.^[15] Besides these effects, it was expected that, in the acetoxylation of toluene, the reaction pressure might also influence the Pd-particle size owing to increased surface coverage.

Moreover, it was speculated by ourselves that larger Pd particles, which were demonstrably present after the synthesis and precursor calcination under an inert-gas (He) atmosphere at high temperature, more or less completely erode and that the more-beneficial smaller Pd particles are formed in an advantageous Pd/Sb ratio. The rationale for this assumption was the fact that 1) pure Pd particles were found in the as-synthesized solids and 2) regardless of the calcination procedure, whether it led to small (2–5 nm) or large (1–2 μm) Pd particles, medium-sized particles (50–100 nm) were present in the above-described Pd/Sb ratio after passing the induction period. In the most-beneficial case, a shortening of the induction period could occur by increasing the reaction pressure.

Herein, we report, for the first time, the marked effect of the reaction pressure (up to 10 bar) on the geometric and electronic structure and the related catalytic performance of a Pd–Sb/TiO₂ catalyst. The aim of this work is to gain deeper insight into the dynamic changes in the surface structure, size, and composition of the Pd particles that occur during the catalytic reaction as a consequence of pressure. Special emphasis is devoted to enhancing the activity and selectivity, along with a shorter induction period.

2. Results and Discussion

2.1. Composition, BET surface area, and phase behavior of the most-active and spent catalysts

The fresh calcined Pd–Sb/TiO₂ solid showed the following composition, as obtained by ICP-OES: 9 wt.% Pd, 12 wt.% Sb. The BET surface area and the pore volume of this sample were found to be 28.6 m²g⁻¹ and 0.1 cm³g⁻¹, respectively. XRD analysis revealed the presence of only metallic Pd in the fresh catalyst (Figure 1). A TEM image of the fresh catalyst showed quite-large Pd particles with sizes that ranged from 1–2 μm (Figure 2). EDX analysis revealed that these particles exclusively contained Pd.

The composition of samples of the most-active and spent catalysts was also studied. However, their composition was close to that of the parent sample, that is, neither a loss of Pd nor of Sb was observed. The BET surface area of the most-active samples revealed a significant increase for those samples at pressures of 1 or 2 bar; this result point to a significant surface-restructuring that occurs during the induction period. At higher reaction pressures, the most-active solids showed surface areas that were close to that of the parent sample. However, the spent samples revealed a significant drop in BET

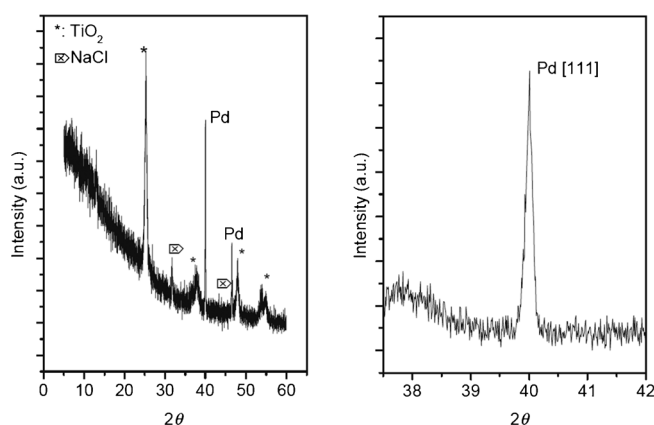


Figure 1. XRD pattern of the parent Pd–Sb/TiO₂ catalyst after calcination under helium.

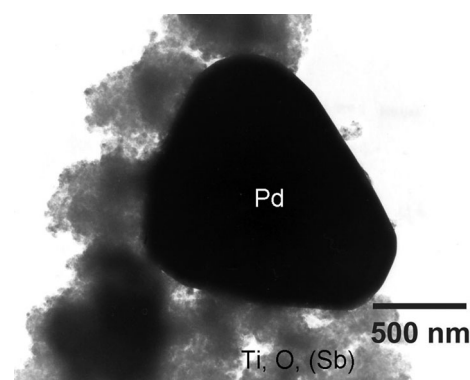


Figure 2. TEM image of big Pd particles (about 1–2 μm) on the surface of the fresh calcined Pd–Sb/TiO₂ catalyst.

surface area with increasing reaction pressure, probably caused by progressive coking (Table 1).

Pressure [bar]	BET-SA [m ² g ⁻¹]	
	Most-active catalyst	Spent catalyst
1	39.4	28.1
2	40.6	25.1
4	27.7	23.8
6	24.8	21.4
8	26.1	12.8

[a] The fresh catalyst has a BET-SA of 28.6 m²g⁻¹.

XRD patterns of the most-active and spent catalysts at different pressures are shown in Figure 3a–d. Reflections that were related to different phases, such as metallic Pd, NaCl (still present from the synthesis), and TiO₂ (support, anatase), were present in all of the samples, irrespective of the applied reaction pressure. However, some changes were observed in the Pd reflections with respect to peak intensity and peak position. In general, all of the patterns of the most-active and spent sam-

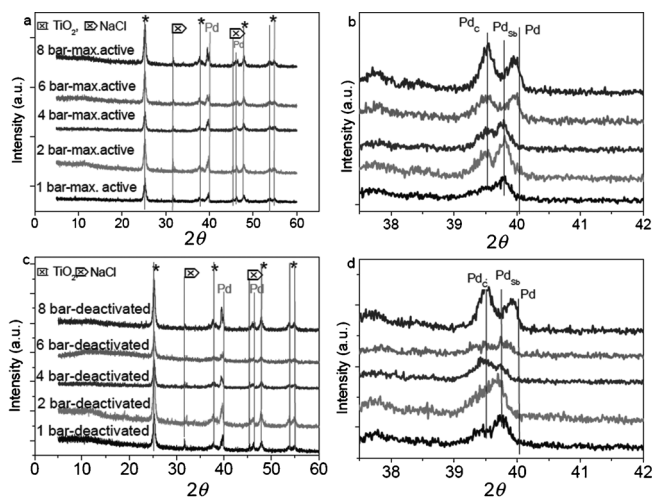


Figure 3. XRD patterns of samples that were treated at different reaction pressures (the parent sample is included for comparison): a) catalysts at their maximum performance; b) most-active samples in the range of the Pd[111] reflection ($2\theta = 38\text{--}41^\circ$); c) spent, deactivated catalysts; and d) these deactivated samples in the range $2\theta = 38\text{--}41^\circ$.

ples revealed a decrease in intensity and/or a shift in the position of the Pd[111] reflection towards lower 2θ values, owing to the incorporation of Sb.^[10] In addition, a shoulder or a second peak at $2\theta = 39.5^\circ$ could be noticed at higher reaction pressures, owing to the growth of a Pd-carbide phase, as observed previously.^[10]

Figure 3b shows the diffractograms of the most-active samples in the range $2\theta = 38\text{--}42^\circ$; there is a clear shift in the Pd reflections compared to the parent sample. Careful examination of the reflections showed that, with an increase in pressure, the shift in the peak position is decreased; that is, a shift in the Pd reflection is much more prominent at 1, 2 and 4 bar compared to the samples at 6 and 8 bar. At higher pressures, Pd tends to exist in its metallic form. XRD patterns of the spent (deactivated) catalysts (Figure 3c) showed no difference in their phase composition compared to the patterns of the most-active samples. However, a shift in the Pd reflection (Figure 3d) was still observed in all of the samples, but with a marginal shift in the solids that were treated at higher pressures.

2.2. Pressure dependence of the catalytic performance

Figure 4 shows the catalytic data after reaching maximum activity, that is, after passing the induction period, and, thus, clearly demonstrates the effect of pressure on the conversion of toluene (X-Tol) and the selectivity for benzyl acetate (S-BA). X-Tol increased from 34 to 75% on increasing the reaction pressure from 1 to 6 bar and then remained constant with further increases in pressure. In a similar way, S-BA also increased to 100% when the reaction pressure was raised to 6 bar and then decreased slightly to 86% with a further increase in pressure. Simultaneously, the pressure showed an additional beneficial effect on the induction period, which was observed to decrease from 11 h (1 bar) to only 3 h (6 bar), as shown in Figure 5. On the other hand, the reaction pressure had shown

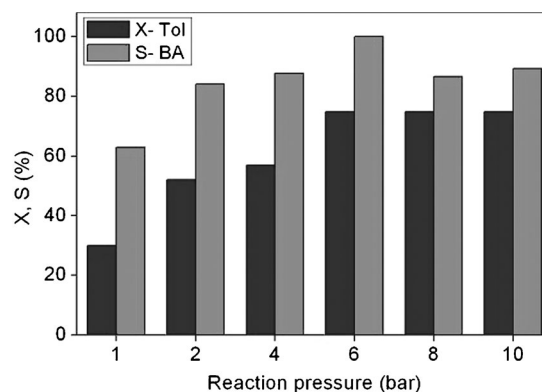


Figure 4. Effect of the reaction pressure on the catalytic performance of the Pd-Sb/TiO₂ catalyst after the induction period, that is, at maximum activity; $T = 210^\circ\text{C}$, molar ratio of Tol/AcOH/O₂/N₂ = 1:4:3:16, GHSV = 2688 h⁻¹ (conversion of toluene: X-Tol, selectivity for benzyl acetate: S-BA).

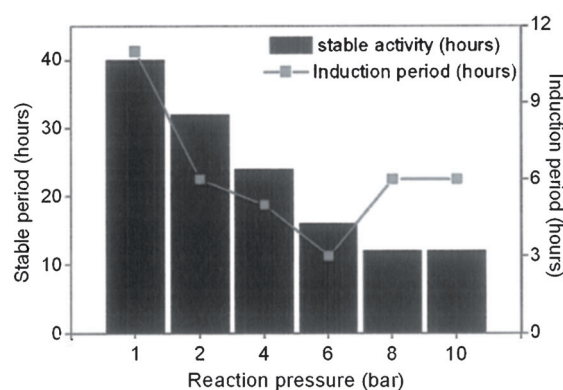


Figure 5. Dependence of the catalyst-induction period and the time of stable operation, including the induction period, on reaction pressure; $T = 210^\circ\text{C}$, $p = 1\text{--}10$ bar, molar ratio of Tol/AcOH/O₂/N₂ = 1:4:3:16, GHSV = 2688 h⁻¹.

some adverse effects on long-term stability, particularly when the pressure was raised to 6 bar and above. In fact, the long-term stability decreased from 40 h at 1 bar to 12 h at 10 bar. However, one should keep in mind that the catalyst was exposed to a tenfold proportion of reactant molecules and its productivity, that is, space-time-yield, increased simultaneously.

Figure 6 and Figure 7 show the time-on-stream changes over up to 12 h with respect to X-Tol and S-BA in more detail. The lowest reaction pressure (1 bar) displayed relatively low initial activity (X-Tol \approx 1%, S-BA \approx 5%), which increased with time-on-stream and reached its maximum (X-Tol = 33%, S-BA = 63%) after an induction period of 11 h. This period seems to be the time required for the Pd particles to transform from 1–2 μm (observed in the fresh solid) into the crucial size of 50–100 nm, which is necessary for improved performance. This increase in size is evident from the TEM measurements (see below). At a pressure of 2 bar, the catalyst also showed a low initial activity (X-Tol \approx 3%, S-BA \approx 10%) that increased steadily with time-on-stream. However, some changes in the induction period, toluene conversion, selectivity for BA, and long-term stability were evident compared to the sample at 1 bar reaction pressure. In this case, the maximum conversion of toluene

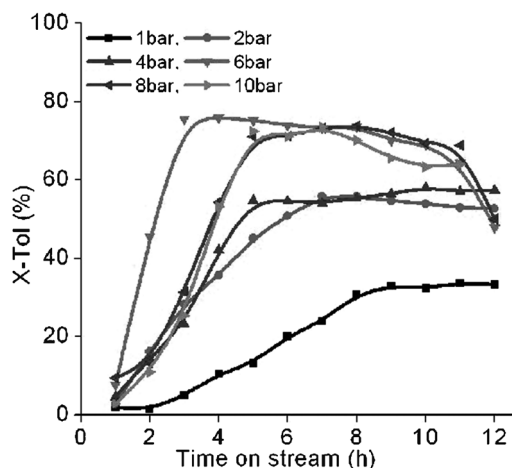


Figure 6. Dependence of a plot of toluene conversion (X-Tol) versus time-on-stream of the Pd-Sb/TiO₂ catalyst on reaction pressure; $T=210^{\circ}\text{C}$, $p=1-10$ bar, molar ratio of Tol/AcOH/O₂/N₂ = 1:4:3:16, GHSV = 2688 h⁻¹.

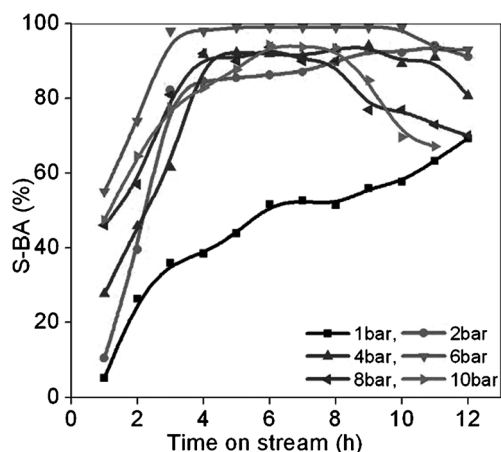


Figure 7. Dependence of a plot of benzyl acetate selectivity (S-BA) versus time-on-stream of the Pd-Sb/TiO₂ catalyst on reaction pressure; $T=210^{\circ}\text{C}$, $p=1-10$ bar, molar ratio of Tol/AcOH/O₂/N₂ = 1:4:3:16, GHSV = 2688 h⁻¹.

rose to 54% and the selectivity for BA reached 89%. In addition, the induction period was halved from 11 h (at 1 bar) to 6 h (at 2 bar). This result indicates that the rate of Pd restructuring is somehow faster at higher pressures. In addition, no considerable deactivation took place up to this pressure. A similar behavior (i.e., low initial activity) was also observed at higher pressures of up to 6 bar, at which the catalyst reached its highest performance. After starting with low activity (X-Tol = 8%, S-BA = 63%), a remarkable conversion of 75% and a selectivity to BA of 100% were obtained within only 3 h on-stream of the induction period. Obviously, the induction period has been shortened significantly from 11 h at 1 bar to only 3 h at 6 bar. It appears that these beneficial effects are due to an acceleration of the changes in the surface, size, and composition of the Pd particles under the influence of pressure, that is, increased surface-reactant concentrations. Such changes on the Pd-Sb/TiO₂ catalysts have also been observed in previous studies,^[10] yet they took much longer.

2.3. In situ XRD analysis of particle restructuring

In previous investigations, we found out that catalysts that contained mixed-metal particles with a Pd/Sb atomic ratio of 5 and a particle size of between 50 and 100 nm showed the highest catalytic performance.^[10] However, these characteristics were only reached after a certain conditioning period, fresh (inactive) catalysts contained pure Pd particles of 1–2 μm.^[10] Clearly, this restructuring of the particles requires a certain time, which depends on the reaction pressure, that is, the concentration of the reactants. Such dynamic behavior of the surface, which includes the dissolution of the parent Pd particles and the formation of mixed Pd-Sb particles with optimum composition and size, was confirmed by an in situ XRD experiment that showed a decrease in the Pd[111] reflection and the growth of a new peak that was assigned to a Pd-Sb phase. Figure 8 shows two patterns from a set of in situ X-ray diffrac-

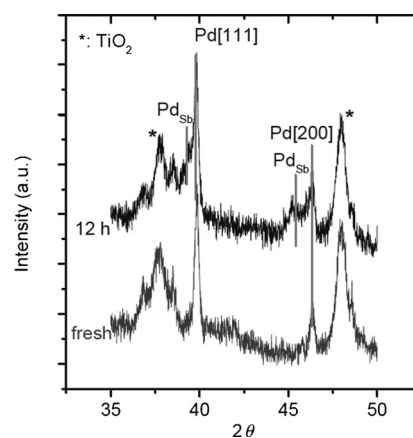


Figure 8. In situ-XRD patterns after the start of the in situ reaction and after 12 h on-stream.

tograms that were obtained under acetoxylation-reaction conditions at 210 °C and ambient pressure in an in situ cell (Anton Paar, XRK900). These patterns reveal a loss of the intensity of both of the Pd reflections (the [111] reflection at $2\theta=40^{\circ}$ and the [200] reflection at $2\theta=46.5^{\circ}$) and the growth of new reflections at slightly lower 2θ values. These reflections can be correlated with an expansion of the Pd lattice, presumably owing to the incorporation of Sb and carbon. Recently, a similar phenomenon of sintering and reactivation of Pt and Rh in automotive-exhaust catalysts was described.^[16] In our case, the beneficial influence of pressure on the restructuring could be observed at pressures of up to 6 bar. Higher pressures (above 6 bar) showed a detrimental effect (Figure 5). Obviously, such reaction pressures, that is, higher surface concentrations of the reactants, hampered an effective desorption of the product. In addition, this increased surface-molecule traffic led to the formation of enhanced oligomers and coke deposition.

As expected, the extent of carbon deposition in the spent samples only marginally increased from 0.043 wt.% h⁻¹ at 1 bar to 0.063 wt.% h⁻¹ at 4 bar. However, a more-pronounced increase, up to 0.25 wt.% h⁻¹, was observed with a further rise in

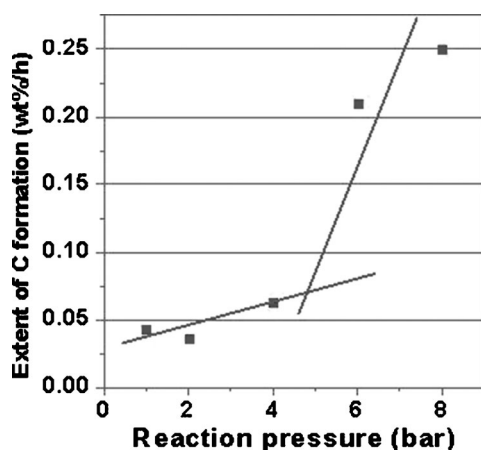


Figure 9. Plot of carbon deposition (wt.% h⁻¹) of the spent samples versus reaction pressure (1–8 bar); *T* = 210 °C, molar ratio of Tol/AcOH/O₂/N₂ = 1:4:3:16, GHSV = 2688 h⁻¹.

pressure to 8 bar (Figure 9). This fact suggests that the higher concentration of carbonaceous compounds on the catalyst surface at higher reaction pressures promotes coke formation and, therefore, deactivation. This coke formation leads to 1) a decrease in BET surface area, 2) a drop in the surface concentration of Pd, and 3) the formation of undesired Pd species (e.g., Pd^{δ-}), owing to interactions between deposited surface coke and surface-Pd species.

2.4. Extended XPS studies of the most-active and spent samples

To gain further insight into the composition and oxidation states of Pd in its nearest-surface region and the dependence of these properties on reaction pressure, XPS analysis was performed on the most-active samples and compared with that of the fresh calcined sample. The Pd 3d XPS spectra revealed the presence of only oxidized Pd species, with a binding energy (B.E.) of 335.8 eV on the surface of this sample (Figure 10), apart from metallic Pd in the bulk sample, as revealed by the XRD studies (see above). However, these oxidized surface species were gradually reduced into metallic Pd during the course of the reaction. As a result, in all of the most-active samples, both oxidized and metallic Pd species co-existed in different proportions, which, again, depended on the reaction pressure. In fact, the presence of both metallic and oxidized Pd species is crucial for obtaining high catalytic performance and also for improving long-term stability.^[17]

Furthermore, the rate of reduction of oxidized PdO into metallic Pd also depends on the reaction pressure, that is, the concentration of organic molecules on the surface that act as reducing agents, such as toluene. Our results show that such reduction occurred at a slower rate at low pressures (≤2 bar; Figure 10). Thus, a significant amount of oxidized PdO species were still found on the surface of the catalysts that were tested at 1 and 2 bar compared to those that were tested at higher pressures. Consequently, the peak for metallic Pd (B.E. = 335.1 eV) was found to increase quite sharply with increasing

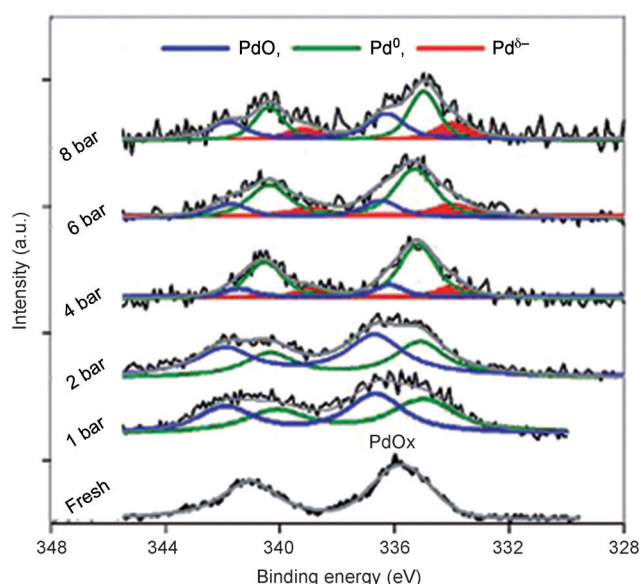


Figure 10. Pd 3d spectra (XPS) that shows PdO, Pd⁰, and Pd^{δ-} species in the near-surface region.

pressure. In addition, a third Pd species was found in the catalysts that were tested at 4 bar and above. This species is a Pd^{δ-} species with a markedly lower binding energy value (B.E. = 333.7 eV) compared to metallic Pd (B.E. = 335.1 eV). As has been reported earlier, the formation of a Pd^{δ-} state is caused by the interactions between surface Pd and deposited carbon species.^[11] The formation of Pd^{δ-} species is typical in catalysts that undergo quick deactivation;^[11] it was not observed in the catalysts that were tested at 1 and 2 bar, which were stable for a longer time (Figure 11). In contrast, the sam-

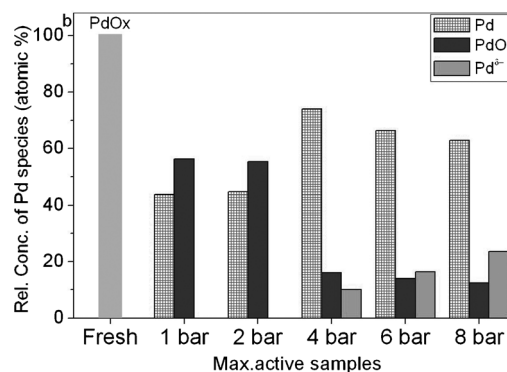


Figure 11. Distribution of different Pd species in the near-surface region as a function of reaction pressure.

ples that were catalytically tested at higher reaction pressures (4–8 bar) contained these undesired Pd^{δ-} species in different proportions. The concentration of Pd^{δ-} species increased with pressure, which is in line with the deactivation behavior of the catalysts.

Furthermore, the Pd/Ti surface-atomic ratios of the most-active samples were found to decrease considerably with an increase in pressure. This result is a consequence of the cover-

ing of the Pd surface by carbon deposits and/or the migration of Pd to deeper layers on-stream, thereby leading to a loss in the surface concentration of Pd, which caused a drop in the catalyst activity with time. However, there was no loss or leaching of Pd from the bulk catalyst, as evidenced by ICP.

2.5. TEM investigation of the morphology and composition of the Pd–Sb particles

Figure 12 shows TEM images of the most-active Pd–Sb/TiO₂ catalysts that were tested at different pressures. The most-active sample from the experiment at 1 bar (11 h on-stream)

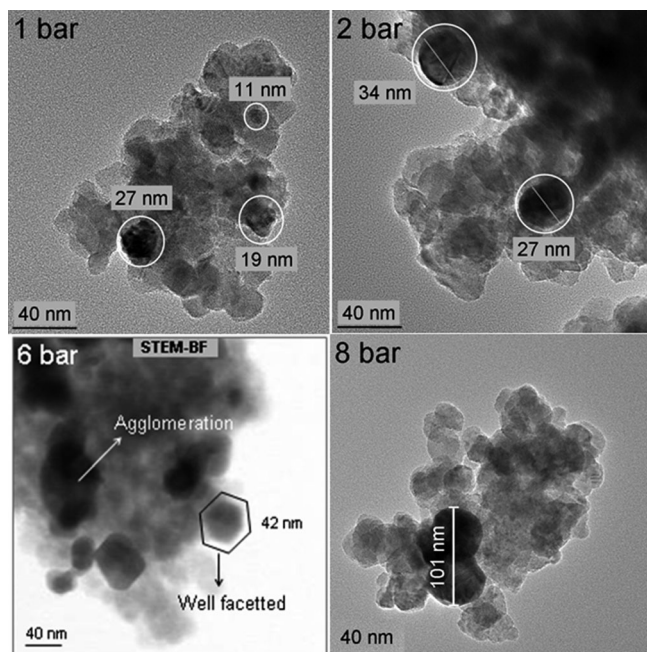


Figure 12. TEM images of the most-active Pd–Sb/TiO₂ solids at different reaction pressures.

only showed particles with sizes of 10–25 nm. An increase in reaction pressure led to increased particle size (about 30 nm at 2 bar, 40–100 nm at 6 bar). This result first was rather strange and hard to understand. Why would the lowest reaction pressure lead to the smallest particles? This question was answered by the in situ XRD experiments, which confirmed the restructuring of the catalyst surface. We now can conclude that, at the start of the treatment, erosion or dissolution of these large Pd particles (1–2 μm) occurred, depending on the reaction pressure, that is, the surface concentration of the reactants. This is a rather slow process at ambient pressure and leads to the smallest particles, but, increasing the pressure to 2 bar sped up the restructuring rate and larger Pd particles (> 30 nm) could be generated after 6 h on-stream. At 6 bar, this size of Pd particles (40–100 nm) was observed within 3 h and this result was similar to the observations at pressures of 8 and 10 bar. These results confirm that a fast collapse of the large initial particles of the fresh catalysts into very small ones occurs during the very initial period on-stream, which is fol-

lowed by a subsequent growth during the induction period, thereby reaching the optimum size and composition faster at higher reaction pressures, up to a maximum of 6 bar. In addition, the mean composition of the particles showed a Pd/Sb ratio of about 5 for those samples that were treated at 1, 2, 4 and 6 bar, whereas a Pd/Sb ratio of about 11 was found for the particles that were treated at 8 bar, which is much higher than the optimum required ratio.^[10]

3. Conclusions

These results provide strong evidence that the reaction pressure, that is, the concentration of reactant molecules on the catalyst surface, has a notable influence on the catalytic activity, product selectivity, space-time-yield of the desired product, induction period, coke deposition, and long-term stability of the catalyst. Catalytic tests were performed at various reaction pressures from 1–10 bar. We found that the catalyst formation was strongly influenced by the reaction pressure, that is, the surface coverage of the active sites by the reactants, intermediates, and products. At a pressure of 6 bar, the highest toluene conversion of 75% and 100% selectivity for benzyl acetate was observed. This result could be due to both a restructuring of the catalyst surface and to the simultaneous formation of active Pd–Sb particles of desired size, composition, and shape during an induction period that is significantly shortened with an increase in pressure. TEM analysis showed an optimum Pd–Sb particle size of 50–100 nm. EDX analysis revealed an optimum Pd/Sb ratio of around 5. XPS confirmed the existence of surface PdO_x and Pd⁰ besides the metallic, bulky Pd that was only seen by XRD. Lastly, in situ XRD showed a decrease in the crystallinity of the large Pd particles in the parent catalyst and the growth of new phases (e.g., Pd–Sb). In summary, these results can inspire the improvement of catalyst compositions and reaction conditions for other partial-oxidation reactions in the near future.

4. Experimental Section

4.1. Catalyst synthesis

The Pd–Sb/TiO₂ catalyst was prepared by impregnation over two steps and by calcination in a He atmosphere at 600 °C for 4 h. The Pd and Sb content were set to 10 and 16 wt.% (nominal), respectively. The calcined solid showed Pd particles with sizes of about 1–2 μm. More details on the catalyst preparation have been reported previously.^[10]

4.2. Characterization of the fresh and spent catalysts

The elemental composition (Ti, Pd, Sb, Na) of the catalysts was determined by using inductively coupled plasma-optical emission spectrometry (ICP-OES) on a Varian 715-ES ICP-emission spectrometer; data analysis was performed with the ICP Expert software. Carbon, hydrogen, nitrogen, and sulfur analysis was performed on a CHNS microanalyzer TruSpec (Leco).

The surface area (BET) and pore-size distribution of the catalysts were determined by using a Nova 4200e device (Quantachrome In-

struments). Before the measurements, the catalyst was evacuated for 2 h at 200 °C to remove any physisorbed water.

Powder X-ray diffraction (XRD) patterns were obtained by using a Stoe STADI P diffractometer that was equipped with a linear position-sensitive detector (PSD) in transmission geometry with $\text{CuK}_{\alpha 1}$ radiation ($\lambda = 1.5406 \text{ \AA}$, 40 kV, 35 mA) in the range $2\theta = 10\text{--}55^\circ$ (step width: 0.25°) under ambient conditions. The time per step was 25 s for the samples without Si as a standard and 160 s with Si as a standard. Processing and assignment of the powder patterns was performed by using the software Win Xpow (Stoe) and the powder diffraction file (PDF) database of the International Centre of Diffraction Data (ICDD).

In situ-XRD studies on the parent Pd–Sb/TiO₂ catalyst were performed by using a Stoe STADI P diffractometer in Bragg–Brentano geometry with CuK_{α} radiation ($\lambda = 1.5418 \text{ \AA}$, 40 kV, 35 mA) and a linear PSD by using a XRK 900 reactor chamber (PAAR, Graz, Austria). The alignment was checked by using a silicon standard. The investigations were performed by heating the sample under an inert atmosphere (He) from ambient temperature to 210 °C, followed by the treatment of the sample at this temperature in an acetic-acid/toluene mixture (molar ratio: 4:1) under a flow of air (30 mL min^{-1}) at ambient pressure. The data were collected in the range $2\theta = 35\text{--}50^\circ$ with a step width of 0.25° and a measurement time of 30 s per step. The phase composition was determined as described above.

TEM measurements were performed at 200 kV by using a JEM-ARM200F (JEOL) device that was aberration-corrected by a CESCOR (CEOS) unit for scanning transmission electron microscopy (STEM) applications. The microscope was equipped with a JED-2300 (JEOL) energy-dispersive X-ray spectrometer (EDXS) for chemical analysis. High-angle annular dark-field (HAADF) and EDXS imaging was operated with a spot size 5c and a 50 μm condenser aperture. For the TEM measurements, the sample was deposited on a holey carbon-supported Cu-grid (300 mesh) and transferred onto the microscope.

X-ray photoelectron spectra (XPS) were recorded by using a VG ESCALAB 220iXL instrument with AlK_{α} radiation ($E = 1486.6 \text{ eV}$). The samples were fixed onto a stainless steel sample holder with double adhesive carbon tape. The peaks were fitted with Gaussian–Lorentzian curves after Shirley background subtraction. The electron-binding energy was referenced to the Ti 2p_{3/2} peak of TiO₂ at 458.8 eV. For quantitative analysis of the near-surface region, the peak areas were determined and divided by the element-specific Scofield factor and the analyzer-dependent transmission function.

4.3. Catalytic tests

Catalytic tests were performed in a fixed-bed Hastelloy-C reactor at 210 °C^[17] and a reaction pressure of 1–10 bar. The molar ratio of Tol/ACOH/O₂/N₂ was set to 1:4:3:16 (GHSV = 2688 h⁻¹; GHSV = gas hourly space velocity).^[17] Product analysis was performed by using off-line GC that was equipped with FID;^[17] this method showed good reproducibility and a relative error of about $\pm 2.5\%$. The calculations of the conversion of toluene (X-Tol) and acetic acid (X-

ACOH) were based on their molar streams at the inlet and the outlet of the reactor. The yields of the formed products (Y) and their selectivities (S) were also calculated from their molar streams. Beside some carbon oxides from total oxidation and BA as the main product, only minor amounts of benzaldehyde (BAL) were observed. The carbon balance was evaluated from unconverted reactants and from the yields of the identified and calibrated products.

In general, the most-active samples were taken out of the reactor after reaching their highest activity and spent samples were taken out after beginning to become deactivated.

Acknowledgements

S.G. would like to thank the Deutsche Forschungsgemeinschaft (grant no. BR-1380/13-1) for financial funding. N.M. acknowledges LIKAT for financial support. The authors would like to thank Dr. M. Schneider for performing the XRD studies.

Keywords: acetoxylation · antimony · gas-phase reactions · palladium · X-ray diffraction

- [1] K. Weissermel, H.-J. Arpe, *Industrielle Organische Chemie*, 5th ed., Wiley-VCH, Weinheim, 1998, p. 252–255.
- [2] F. Calaza, D. Stacchiola, M. Neurock, W. T. Tysoe, *J. Am. Chem. Soc.* **2010**, *132*, 2202–2207.
- [3] E. Benazzi, C. J. Cameron, H. Mimoun, *J. Mol. Catal.* **1991**, *69*, 299–321.
- [4] L. Ebersson, E. Jonsson, *Acta Chem. Scand. Ser. B* **1974**, *28*, 771–778.
- [5] T. Komatsu, K. Inaba, T. Uezono, A. Onda, T. Yashima, *Appl. Catal. A* **2003**, *251*, 315–326.
- [6] L. Ebersson, L. G. Gonzalez, *Acta Chem. Scand.* **1973**, *27*, 1249–1254.
- [7] K. Bauer, D. Garbe, H. Surburg, *Ullmann's Encyclopaedia of Industrial Chemistry*, VCH, Weinheim, A 11, 1988, 141.
- [8] V. N. Kalevaru, A. Benhmid, J. Radnik, M. M. Pohl, U. Bentrup, A. Martin, *J. Catal.* **2007**, *246*, 399–412.
- [9] A. Benhmid, K. V. Narayana, A. Martin, B. Lücke, S. Bischoff, M. M. Pohl, J. Radnik, M. Schneider, *J. Catal.* **2005**, *230*, 420–435.
- [10] S. Gatla, N. Madaan, J. Radnik, V. N. Kalevaru, M. M. Pohl, B. Lücke, A. Martin, A. Brückner, *Appl. Catal. A* **2011**, *398*, 104–112.
- [11] J. Radnik, A. Benhmid, V. N. Kalevaru, M.-M. Pohl, A. Martin, B. Lücke, U. Dingerdissen, *Angew. Chem.* **2005**, *117*, 6929–6933; *Angew. Chem. Int. Ed.* **2005**, *44*, 6771–6774.
- [12] V. N. Kalevaru, A. Benhmid, J. Radnik, B. Lücke, A. Martin, *J. Catal.* **2006**, *243*, 25–35.
- [13] F. M. T. Mendes, F. B. Noronha, C. D. D. Souza, M. A. P. da Silva, A. B. Gaspar, M. Schmal, *Stud. Surf. Sci. Catal.* **2004**, *147*, 361–366.
- [14] C. D. Chang, W. H. Lang, R. L. Smith, *J. Catal.* **1979**, *56*, 169–173.
- [15] M. Forissier, M. Formenti, J. R. Bernard, *Catal. Today* **1991**, *11*, 73–83.
- [16] H. Hirata, K. Kishita, Y. Nagai, K. Dohmae, H. Shinjoh, S. Matsumoto, *Catal. Today* **2011**, *164*, 467–473.
- [17] N. Madaan, S. Gatla, V. N. Kalevaru, J. Radnik, B. Lücke, A. Brückner, A. Martin, *J. Catal.* **2011**, *282*, 103–111.

Received: July 31, 2012

Published online on October 26, 2012